

## Morphology and Properties of Poly(oxymethylene) Engineering Plastics

*Tatiana Sukhanova,\*<sup>1</sup> Vladimir Bershtein,<sup>2</sup> Mimi Keating,<sup>3</sup> Galina Matveeva,<sup>1</sup> Milana Vylegzhanina,<sup>1</sup> Victor Egorov,<sup>2</sup> Nina Peschanskaya,<sup>2</sup> Pavel Yakushev,<sup>2</sup> Edmund Flexman,<sup>3</sup> Stefan Greulich,<sup>3</sup> Bryan Sauer,<sup>3</sup> Kathleen Schodt<sup>3</sup>*

<sup>1</sup> Institute of Macromolecular Compounds of the Russian Academy of Sciences, 31 Bolshoj Pr. V.O, 199004 St. Petersburg, Russia

E-mail: xelmic@imc.macro.ru

<sup>2</sup> Ioffe Physico-Technical Institute of the Russian Academy of Sciences, 26 Politechnicheskaya Str, 194021 St. Petersburg, Russia

<sup>3</sup> E.I. du Pont de Nemours & Company, Experimental Station, Wilmington, DE 19880 323, USA

**Summary:** Comparative WAXD/SAXS/SEM/DSC structural studies of a series of semi-crystalline poly(oxymethylene) (POM) engineering plastics, including the commercial products, homopolymer Delrin<sup>®</sup> and typical poly(oxymethylene-co-oxyethylene)s, and a few lab-made POM compositions, were performed. The latter differed in their content of functional additives (present in low concentrations) and POM molecular weight characteristics. In parallel, their densities, thermal behavior/laser-interferometric creep rate spectra (DSC/CRS) at 20-180 °C, as well as long-term creep resistance (LTCR) at 20 °C were studied. It has been found that introducing the nucleating agents and oxyethylene units resulted in formation of more fine spherulitic or practically non-spherulitic structure with close- or loose-packed lamellar stacks. The presence of both "thick" (5-10 nm) and "thin" (1.5-3 nm) lamellae in the weight ratio of ~3:1 was shown in all cases. Close values of real POM crystallinities, not exceeding 50%, were obtained by WAXD and DSC. A predominant role of "straightened out" or slightly bent tie chains in disordered layers of isotropic POMs was presumed, resulting in segmental dynamics differently constrained by crystallites (DSC/CRS data). As a result, certain morphology –density –creep resistance correlations were found.

**Keywords:** creep; molecular dynamics; morphology; polyethers; thermal properties

### Introduction

Poly(oxymethylene) (POM) homo- and copolymers are important engineering plastics. High POM chain flexibility and symmetry cause their fast crystallization, and complicated morphology and dynamics at 150-430 K<sup>[1-7]</sup>. Of most significance for POM engineering properties is the

segmental dynamics within disordered regions over the  $T_g$ - $T_m$  range, at  $\sim 300$ - $400$  K, which is differently constrained by crystallites. Detailed analysis of dynamics in POMs was recently performed by the combined use of DSC and laser-interferometric creep rate spectroscopy (CRS)<sup>[6, 7]</sup>.

The morphological studies have shown that the spherulitic structure is typical of the melt crystallized POM<sup>[8-10]</sup>. Using AFM<sup>[5]</sup>, PLM and TEM<sup>[8-10]</sup>, the changes in the crystalline morphology of POM, oriented POM and its blends during crystallization and melting processes have been investigated.

The objective of this study was to understand the influence of the presence of low concentrations of ethylene oxide content in chains or the addition of nucleating agents, and the influence of a decrease in molecular weight on morphology, lamellar textures, thermal properties and creep resistance in molded POM homo- and copolymers. It was intended to reveal structure/properties correlations within a series of commercial products and lab-made compositions.

## Experimental

Table 1. POM samples studied

Sample	$M_n$	$M_w/M_n$	Nucleating
Delrin® IIP	$7.6 \cdot 10^4$	1.84	Nucleated
Delrin 6-1	$7.6 \cdot 10^4$	1.84	No nucleating agent
Delrin 6-2	$7.6 \cdot 10^4$	1.84	No nucleating agent, minimum amounts of additives
Delrin 6-3	$7.6 \cdot 10^4$	1.84	Nucleated
Delrin 6-4	$5.5 \cdot 10^4$		No nucleating agent
Delrin 6-5	$7.6 \cdot 10^4$	1.84	Nucleated
Celcon M15HP	$1.5 \cdot 10^4$	7.47	Nucleated
Celcon M25	$8.4 \cdot 10^3$	14.7	Nucleated

Note. Delrin 6-1 – 6-5 samples are the lab-made compositions. Celcons are POMs with 0.4 mol % (Celcon M15HP) or 1.4 mol% (Celcon M25) ethylene oxide units.

A series of POM samples, including the commercial homopolymer Delrin® IIP, copolymers

Celcon M15HP and Celcon M25, and lab-made POM variations (Table 1), were studied. The latter differed in terms of the functional additives (nucleating agents, process aid, antioxidant) introduced in concentrations less than 1 wt.-%, and by POM molecular weight and MWD. The samples were obtained by injection molding, under pressure of 1 000 bar, with cooling at the rate of 200 K min<sup>-1</sup>.

Comparative WAXD/SAXS/SEM/DSC structural studies of the materials were performed. In parallel, their densities, thermal behavior/laser interferometric creep rate spectra (DSC/CRS) at 20-180 °C as well as long-term creep resistance (LTCR) at 20 °C, were studied.

The morphology of samples was studied by scanning electron microscopy (SEM). Before SEM observation, samples were etched using the permanganic etching technique<sup>[13]</sup>. The etched surfaces were sputter coated with a very thin layer of gold (~15 nm thick) to prevent charging during imaging (SCD 050 ion-sputtering device, BALZERS, Switzerland) and were examined with a CamScan MV2300D scanning electron microscope at 15 kV at magnifications from X 500 to X 10 000. X-ray measurements were performed on a DRON-3 diffractometer using Ni-filtered CuK<sub>α</sub> irradiation. DSC curves were measured using the Perkin-Elmer DSC-2 apparatus, under nitrogen or helium atmosphere, at the heating rates of 2.5-20 K min<sup>-1</sup>. The CRS method is based on precise measuring of low creep rates as a function of temperature by using a laser interferometer based on Doppler effect<sup>[11, 12]</sup>. In this research, the CRS setup, operating under uniaxial compression, was used.

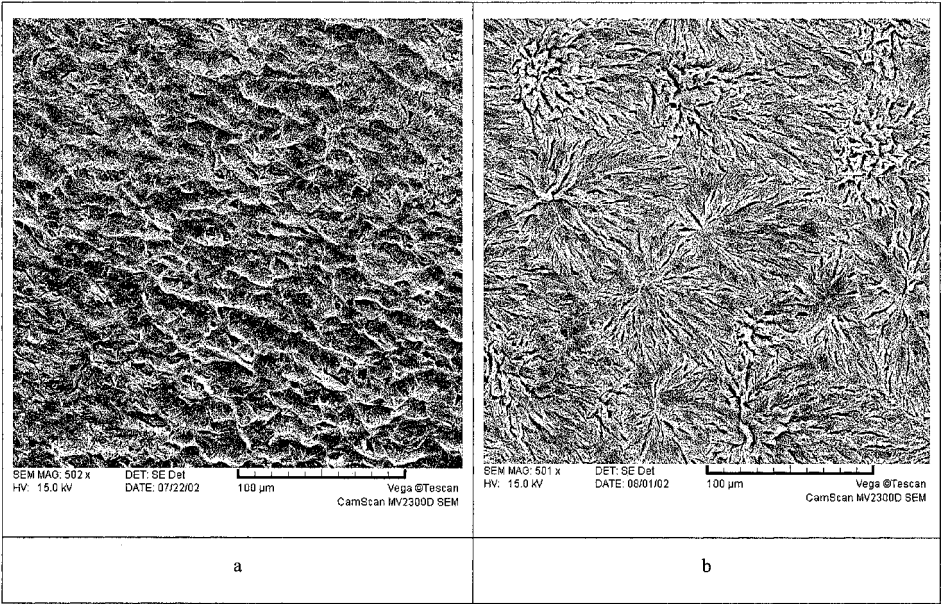
## Results and Discussion

### *Morphology*

SEM investigations revealed very marked differences in POM morphologies depending on their composition. The majority of the lab-made specimens exhibited well-defined large- or fine-spherulitic morphology (Figure 1 b,c). However, Delrin 6-3 and commercial samples, Delrin<sup>®</sup>IIP (Figure 1a) and Celcon M25 (Figure 1d), did not manifest a distinct spherulitic morphology. Delrin 6-3 and Delrin<sup>®</sup>IIP consisted of close-packed lamellar stacks. Celcon M25 exhibited the

hedritic morphology. On the whole, lamellar stacks in the samples studied had thicknesses ranging from 0.2 to 5  $\mu\text{m}$ . The maximum thickness of 1.8-5.4  $\mu\text{m}$  was found for Delrin 6-3.

Estimation of the average spherulite diameter has shown that introducing the nucleating agents resulted in the formation of fine spherulites ( $D_{\text{sph}} \approx 20 \mu\text{m}$ , Delrin 6-5, Figure 1c) or practically non-spherulitic structure (Delrin 6-3). On the other hand, non-nucleated Delrin 6-2 displays two populations of spherulites with the average diameters of 110 and 55  $\mu\text{m}$  (Figure 1b). Copolymers Celcon M25 and Celcon M15HP distinctly showed more loose-packed lamellar morphologies



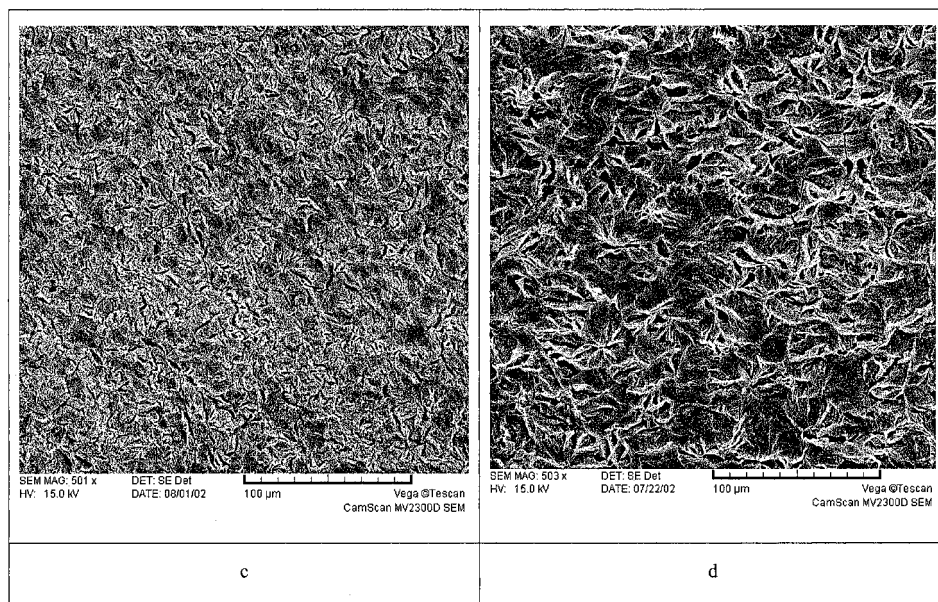


Figure 1. SEM images of the etched cut surfaces of the samples Delrin<sup>®</sup> IIP (a), Delrin 6-2 (b), Delrin 6-5 (c) and Celcon M25 (d). Magnification: x500.

than homopolymers (Figure 1d), in accordance with their essentially lower densities (Table 2). On the contrary, Delrins 6-3 and 6-5 had the maximum densities.

### *Crystalline structure*

Structure parameters, estimated by WAXD, SAXS and DSC, and the measured densities are listed in Table 2. In the WAXD profiles of all the samples studied, three typical reflections were observed corresponding to  $2\theta = 10.0\text{--}10.2^\circ$ ;  $23.2^\circ$  (strong), and  $34.5\text{--}34.7^\circ$ . WAXD data were indexed in terms of the most probable hexagonal unit cell with  $a = 4.42 \text{ \AA}$ , and  $c = 17.48 \text{ \AA}$ .

Table 2. Structure parameters estimated by WAXD, SAXS, DSC and densitometry data.

Sample	$L_c$	$L_{ab}$	$X_{WAXD}$	$X_{DSC}$	$l_c$	$L_B$	$\rho$
No.	nm	nm	%	%	nm	nm	g/cm <sup>3</sup>
Delrin <sup>®</sup> IIP	2.3±0.2	13	46	51±3	9.5±0.5	21.1	1.4197
Delrin 6-1	2.3±0.2	10.5	43	50±3	9.5±0.5	18.9	1.4180
Delrin 6-2	1.8±0.2	13	24-38	49±3	10,0±0,5	18.2	1.4235
Delrin 6-3	1.6±0.2	17.5	46-54	50±3	10.5±0.5	18.2	1.4260
Delrin 6-4	2.2±0.2	15	30-47	49±3	9.5±0.5	19.6	1.4206
Delrin 6-5	1.5±0.2	7	39-50	49±3	10.5±0.5	*	1.4245
Celcon M15HP	2.0±0.2	13	48	48±3	6.5±0.5	17.0	1.4107
Celcon M25	3.0±0.2	20	42	45±3	4.5±0.5	19.6	1.4001

The gyration radii of the scattering domains  $R_g$  ranged from 2.8-3.0 nm for Celcons to 3.10 nm (Delrin 6-1 and 6-4), and to 3.33 nm (Delrin<sup>®</sup> IIP). The maximum value of the long period  $L_B = 21.1$  nm has also been observed for the commercial Delrin<sup>®</sup> IIP. It should be noted that a long period could not be discerned for Delrin 6-5. Combined WAXD/SAXS/DSC analysis indicated the presence of both “thick” ( $l_c = 5$ -10 nm, DSC data) and “thin” ( $l_c = 1.5$ -3 nm, WAXD data) lamellar crystallites in the POMs studied. Close real values of POM crystallinities (see below) were obtained from both WAXD and DSC estimates. A large spread of  $X_{WAXD}$  values was obtained for Delrin 6-2 and Delrin 6-4 only, obviously associated with their large-spherulitic morphology.

## Properties

The DSC approach used to analyse POM segmental dynamics and true melting characteristics was similar to that described elsewhere<sup>[6, 7]</sup>. It included, in particular, the estimation of the effective activation energy  $Q$  of segmental motion as a function of temperature, and “parameter of intrachain cooperativity of melting”  $\nu$ , characterizing the length of stereoregular sections in chains<sup>[14]</sup>.

It was found that the endotherm, extending from  $\sim 323$  to  $453$  K on the DSC curves of POMs, must be subdivided into three temperature ranges relating to: melting of basic, “thick” lamellae (thickness  $l_c \approx 5$ - $10$  nm,  $\sim 433$ - $453$  K); melting of “thin” lamellae ( $L_c \approx 1.5$ - $3$  nm,  $413$ - $433$  K), and the endotherm associated with a gradual “unfreezing” of segmental dynamics within the interlamellar, disordered layers (at  $\sim 323$ - $413$  K). In all cases, the weight ratio of “thick” and “thin” lamellae was equal to  $\sim 3:1$ .

The found values of the parameter  $\nu \approx (2-4)l_c$  indicated the predominant role of “straightened out” and slightly bent tie chains in intercrystalline layers of isotropic POMs that might imply their constrained dynamics. Really, the “usual” cooperative glass transition ( $T_g = 250$ - $260$  K) was strongly suppressed whereas, depending on the thermal treatment regime, a heat capacity step as a feature of glass transition-like behavior could arise on the DSC curve at any temperature over the  $\sim 300$ - $400$  K range. By scanning at different scanning rates, the  $Q(T)$  dependencies were estimated.

The pronounced  $Q(T)$  dispersions were found, indicating large heterogeneity of segmental dynamics over the  $T_g$ - $T_m$  range. Thus, Figure 2 shows that  $Q$  values range from  $\sim 150$  to  $600$  kJ/mol under these conditions. This was interpreted in terms of the variable constraining influence of crystallites on segmental motion in tie chains due to their “anchoring” to the rigid crystalline constraints and some difference in the conformational state of chains. Larger deviations of the activation energies from the Arrhenius  $Q(T)$  line corresponded to the stronger constraining effect. Figure 2 shows that the latter is more pronounced in the close-packed Delrin<sup>®</sup> IIP than in loose-packed Celcon M25.

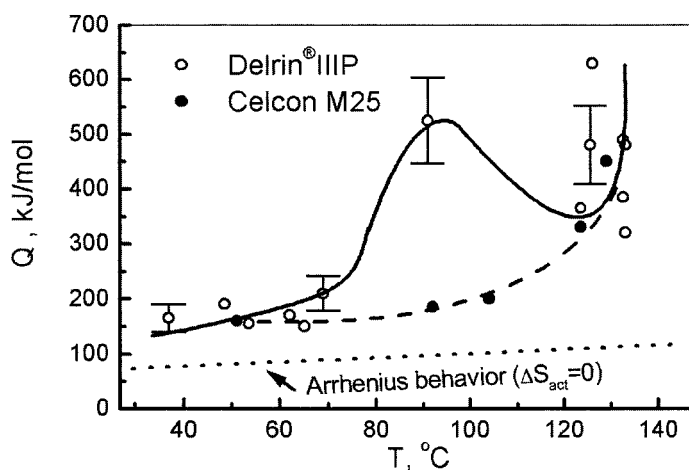


Figure 2. Activation energy of segmental motion versus temperature plots estimated by DSC for Delrin® IIP and Celcon M25 over the  $T_g - T_m$  range. Dotted line corresponds to Arrhenius relation, i.e. to noncooperative relaxation processes, at frequency of  $10^{-2}$  Hz.

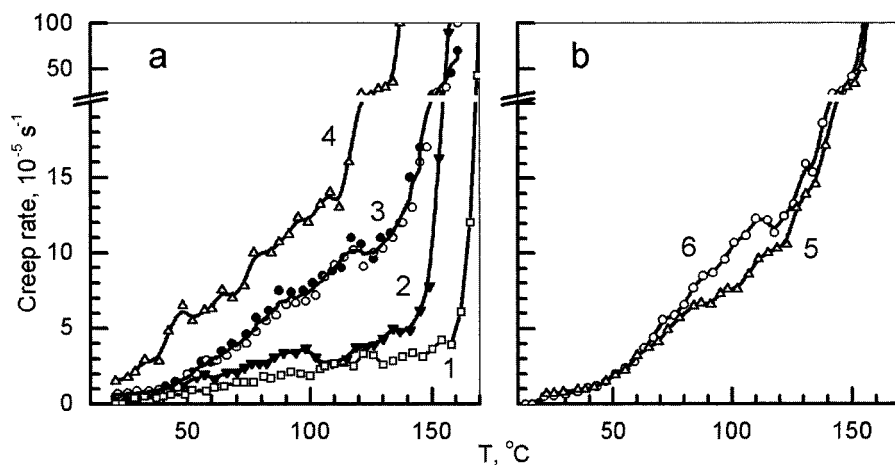


Figure 3. CR spectra obtained for (a) commercial POM plastics, Delrin® IIP (1, 3) and Celcon M25 (2, 4), and (b) lab-made Delrin compositions with (6-5 sample, curve 5) or without (6-2 sample, curve 6) nucleating agents. Curve 3 indicates reproducibility for two identical samples. Compression, 10 s, 3 MPa (curves 1 and 2) or 10 MPa (curves 3-6).



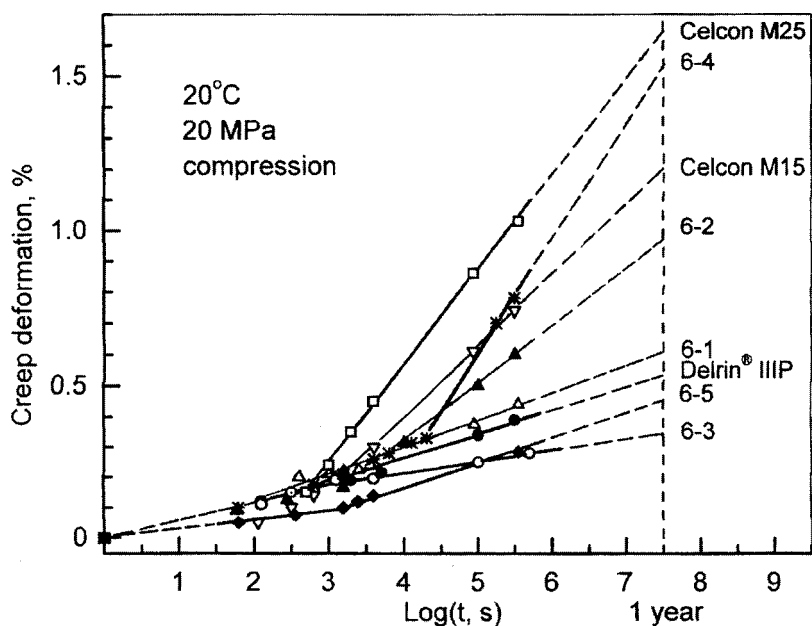


Figure 4. Long-term creep resistance: Comparative POM creep deformation versus logarithm time dependencies.

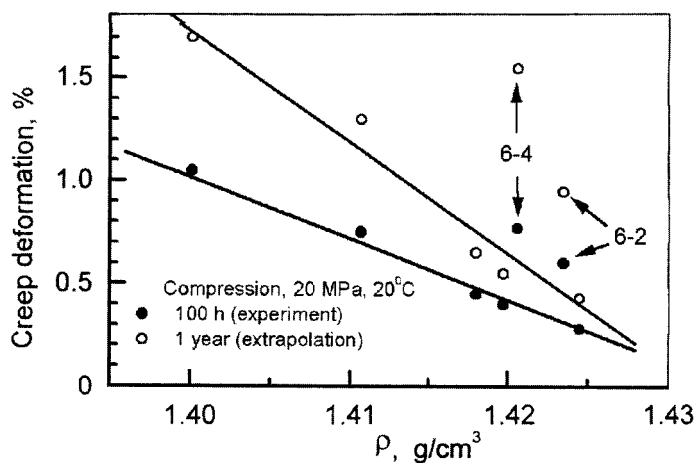


Figure 5. Long-term creep resistance: POM creep deformation versus density dependencies.

The discrete creep rate spectra, with numerous CR peaks in their complicated contours, have previously been obtained under tension for a series of POM compositions<sup>[6,7]</sup>. These demonstrated both dynamic heterogeneity within the temperature regions of  $\beta$ - and  $\alpha$ -relaxations and increasingly constrained segmental relaxations at elevated temperatures. Moreover, it was shown that different small additives affected the CR spectrum.

In this work, the CR spectra, consisting of a few strongly overlapping peaks, were obtained for POMs studied under compression over the 293-443 K range. These spectra also demonstrated a gradual “unfreezing” of differently constrained segmental motions in the interlamellar layers. The spectra of the samples given in Table 1 differed substantially, especially at intermediate temperatures far from both  $T_g$  and  $T_m$ . Figure 3 illustrates the different relaxation behaviors of commercial Delrin<sup>®</sup>IIP and Celcon M25 (a), and the influence of nucleating agent (b). Really, less constraining effect in Celcon than in Delrin (compare with Figure 2) results here in the displacement of the Celcon spectrum by 303-313 K to lower temperatures, i.e., lesser creep resistance at elevated temperatures. Besides, the Celcon spectrum was more sensitive to an increase in stress (Figure 3a). Better behaviour at elevated temperatures was attained in POM due to introducing the nucleating agent, e.g., for the “fine-spherulitic” 6-5 sample compared to that for the non-nucleated, “large-spherulitic” 6-2 sample (Figure 3b).

Finally, the POM compositions studied differed in terms of their long-term creep resistance, even at room temperature, and a certain LTCR versus morphology correlation was found. Figure 4 shows that LTCR increases in the following order. Celcons with loose-packed morphology and large MWD — non-nucleated, “large-spherulitic” Delrins 6-2 and 6-4, with minimum amounts of additives or with the lower molecular weight, respectively, - non-nucleated, “large-spherulitic” Delrin 6-1 - close-packed, nucleated Delrin<sup>®</sup>IIP - nucleated Delrin 6-3 and 6-5 compositions with fine or practically non-spherulitic morphologies. Figure 5 shows linear correlation (inverse proportionality) found between LTCR and POM density. Anomalous high creep was observed here only for Delrin 6-4 and Delrin 6-2.

## Conclusion

The combined study performed allowed us to determine the differences in morphology of a series of POM (commercial and lab-made) engineering plastics and their correlations with the properties. Advantages of POM homopolymers compared to the copolymers and the positive role of some small additives in the formation of finer morphology and better creep resistance.

## Acknowledgements

This work was supported by Du Pont and CRDF RP1-546-ST-02 project.

- [1] N. G. McCrum, B. E. Read, G. W. Williams, *Anelastic and Dielectric Effects in Polymeric Solids*, Wiley, New York 1967.
- [2] R. J. Højfors, E. Baer, P. H. Geil, *J. Macromol. Sci., Phys.* **1977**, *13*, 323.
- [3] M. Y. Keating, B. B. Sauer, E. A. Flexman, *J. Macromol. Sci., Phys.* **1997**, *36*, 717.
- [4] B. B. Sauer, P. Avakian, E. A. Flexman, M. Y. Keating, B. B. Hsiao, R. K. Verma, *J. Polym. Sci., Part B: Polym. Phys.* **1997**, *35*, 2121.
- [5] B. B. Sauer, R. S. Mclean, D. J. Londono, *J. Macromol. Sci., Phys.* **2000**, *39*, 519.
- [6] V. A. Bershtein, L. M. Egorova, V. M. Egorov, N. N. Peschanskaya, P. N. Yakushev, M. Y. Keating, E. A. Flexman, R. J. Kassal, K. P. Schodt, *J. Macromol. Sci., Phys.* **2002**, *41*, 797.
- [7] V. A. Bershtein, L. M. Egorova, V. M. Egorov, N. N. Peschanskaya, P. N. Yakushev, M. Y. Keating, E. A. Flexman, R. J. Kassal, K. P. Schodt, *Thermochim. Acta* **2002**, *391*, 227.
- [8] M. Jaffe, B. Wunderlich, *Kolloid. Z.Z. Polym.* **1967**, *216-217*, 203.
- [9] K. O'Leary, P.H. Geil, *J. Macromol. Sci., Phys.* **1967**, *1*, 147.
- [10] B. Wunderlich, *Macromolecular Physics*, 1-3, Academic Press, New York 1980.
- [11] N. N. Peshanskaya, P. N. Yakushev, A. B. Sinani, V. A. Bershtein, *Thermochim. Acta* **1994**, *238*, 429.
- [12] N. N. Peschanskaya, P. N. Yakushev, A. B. Sinani, V. A. Bershtein, *Macromol. Symp.* **1997**, *119*, 79.
- [13] R.H. Olley, D.C. Bassett, *Polymer* **1982**, *23*, 1707.
- [14] V. A. Bershtein, V. M. Egorov, *Differential Scanning Calorimetry. Physics, Chemistry, Analysis, Technology*, Ellis Horwood, New York 1994.

